J. Fluid Mech. (1990), *vol.* 212, *pp.* 25–39
Printed in Great Britain

The bifurcation of liquid bridges

By D. H. PEREGRINE, G. SHOKER† AND A. SYMON†
School of Mathematics, University Walk, Bristol BS8 1TW, UK

(Received 16 May 1989)

Details of the shape of the liquid bridge joining a nascent water drop to its parent body are presented for times before, after and at the instant of bifurcation when the drop is created and also when the secondary droplet is formed. After the instant of bifurcation there is 'unbalanced' surface tension which gives an impulse to the rest of the fluid causing strong surface deformations. The major point of this work is to draw attention to the strong up–down asymmetry at each bifurcation point. The geometric similarity at each bifurcation instant supports the conjecture that the flow converges to just one similarity solution of the type described by Keller & Miksis (1983) in which only surface tension and inertia are important. Features of the flow before and after bifurcation are discussed.

1. Introduction

We describe an exploratory study of the fluid motion associated with the breaking of a liquid bridge. This breaking most commonly occurs when drops form. The last thin connection with the parent body of liquid is the liquid bridge which parts to create two separate masses. We focus attention on the neighbourhood in space and time of the point at which this bifurcation occurs in low-viscosity liquid. Photographs are presented illustrating the formation of water drops.

Drop formation and associated free surface phenomena such as splashes have been studied photographically for one hundred years. Particularly noteworthy contributors are Rayleigh (1891), Worthington (e.g. 1897, 1908) and Edgerton (e.g. Edgerton, Hauser & Tucker 1937). More recent examples include studies of drop formation from a liquid jet such as Goedde & Yuen (1970), and Chaudhary & Maxworthy (1980*a*, *b*). Marschall (1985) has useful photographs of drops in a liquid–liquid system. However, the majority of studies have tended to concentrate on the number, size and trajectory of drops formed in various circumstances.

Theoretical study has followed a number of directions. Studies of the static stability of pendent drops (e.g. Pitts 1974) indicate when drops will form, as do studies of the stability of liquid cylinders. These latter have been carried further to clarify the evolution of this instability (e.g. Chaudhary & Redekopp 1980), but not all the way to bifurcation. Meseguer & Sanz (1985) develop a one-dimensional model for liquid-bridge dynamics and make comparison with experiments on neutrally buoyant bridges. For *viscous* flow Wilson (1988) gives a simple model of dripping, but more considerable notice has been given to the break-up of large drops into small drops by an outer viscous straining flow. Taylor (1932) drew attention to this type of flow. Recent work of Stone & Leal (1989) describes this drop bifurcation with a numerical model which gives a good simulation of experiments (Stone, Bentley &

† Please address correspondence to D. H. Peregrine. G. Shoker and A. Symon were undergraduates in the Physics Dept., Bristol University at the time the experiments were performed.

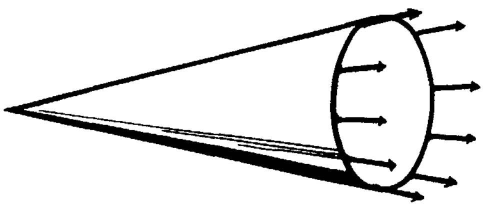

FIGURE 1. Capillary forces on the tip of a conical region of fluid of length r and half-angle α. Total force due to surface tension is $2\pi r \sin\alpha T$, yet the mass of fluid is $\frac{1}{3}\rho\pi r^3 \sin^2\alpha \cos\alpha$, so that as $r \to 0$ the acceleration becomes singular like r^{-2}.

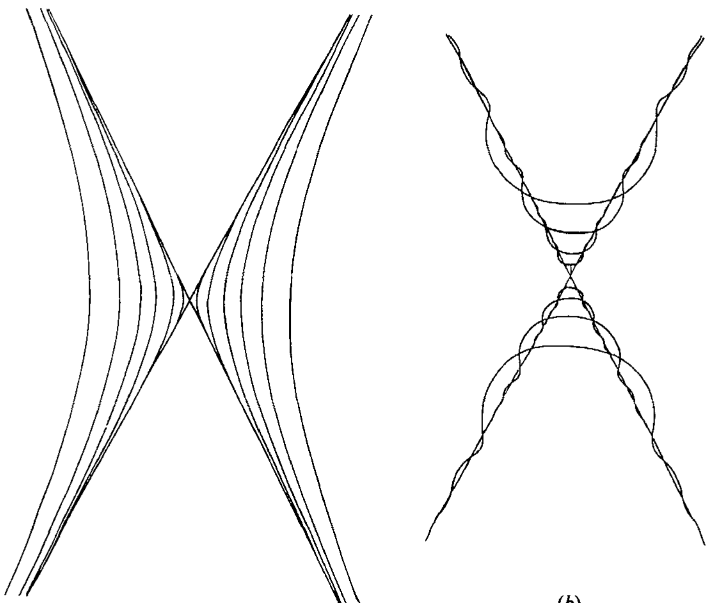

FIGURE 2. A sketch of possible self-similar shapes (a) for flow approaching bifurcation, (b) for flow after bifurcation.

Leal 1986). However, the motion at bifurcation is too rapid and on too small a scale to model accurately.

The only paper which is concerned with effectively *inviscid* motion close to bifurcation is Keller & Miksis (1983): it prompted the experiments described here. Keller & Miksis consider flow governed solely by surface tension and inertia in circumstances where no lengthscale is present. For example, cases where the geometry is fully specified by angles such as occurs if an initial condition is simply a cone or a wedge. Keller & Miksis (1983) argue that such flows are self-similar since if surface tension, T, and density ρ, are the only relevant dimensional quantities, then a lengthscale, $(Tt^2/\rho)^{\frac{1}{3}}$, and a velocity scale, $(T/\rho t)^{\frac{1}{3}}$, can only be found by combining them with time t. These scales indicate the nature of the velocity singularity which occurs at an initial time for conical geometry owing to surface tension forces being 'unbalanced' at the apex. See figure 1. Keller & Miksis give computed solutions for the self-similar deformation of wedges of liquid.

The relevance of such a model to any particular flow can be judged by introducing other physical properties. For example, kinematic viscosity, ν, permits evaluation of a viscous lengthscale, $L_\nu = \rho\nu^2/T$. For water at 20 °C, $L_\nu = 14 \times 10^{-9}$ m which spans

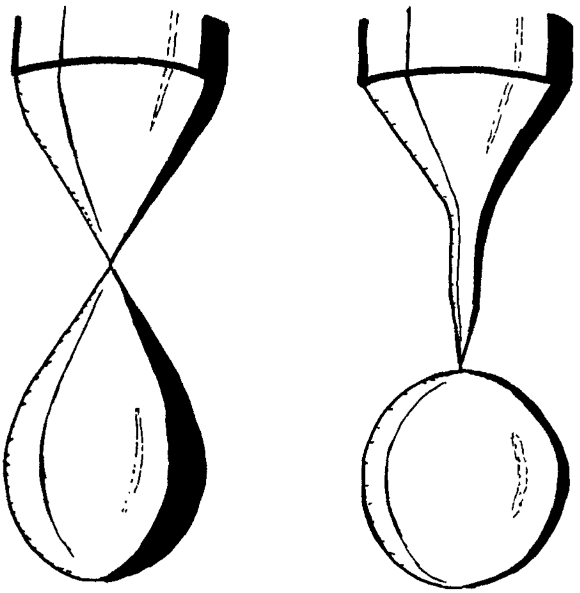

FIGURE 3. (a) Naive view of drop formation. (b) Sketch of observed drop formation.

only a few molecules. The similarity lengthscale equals L_ν when $t = 1.9 \times 10^{-10}$ s and the similarity velocity is then 73 m s^{-1}. Additional comparison of this last figure with the velocity of sound suggests that compressibility is unimportant. Thus for low-viscosity liquids, like water, it appears that inviscid modelling with capillary forces is relevant. The dimensional argument applies equally to two fluids, i.e. liquid–gas or liquid–liquid systems, so that the only macroscopic parameters for these self-similar flows are surface tension, density ratio across the interface and geometrical angles and ratios.

A self-similar model can describe bifurcation, not only for the flow after the bifurcation instant where two independent cones of liquid occur at $t = 0$, but also before bifurcation where the flow is approaching conical geometry as time approaches $t = 0$ from below. Figure 2 gives a sketch of the solutions that are envisaged.

Irrotational flow is usually a good approximation for low-viscosity flow starting from rest. The singular rates of strain, $O(t^{-1})$, inherent in the self-similar singularity are only likely to amplify vorticity that corresponds to a pre-existing swirl. The shears and rates of strain in much drop formation do not exceed m s^{-1}/mm corresponding to a timescale of a millisecond. Although precise timing is not available for the photographs shown here, the local bifurcation events had an overall time span of about 100 μs. This supports the notion that larger-scale motions are unimportant and that the flow is irrotational and likely to be self-similar. The exceptional case of a flow with swirl suggests an interesting line of further study especially for weak swirl.

A naive view of drop formation would give the classical 'tear drop' shape with bifurcation occurring at the apex of a pair of cones, as sketched in figure 3. However, as our photographs show, this is not the case and for water drops forming in air the configuration is sketched in figure 3(b). The marked lack of up–down symmetry near the bifurcation point does not appear to have been remarked upon before. The same

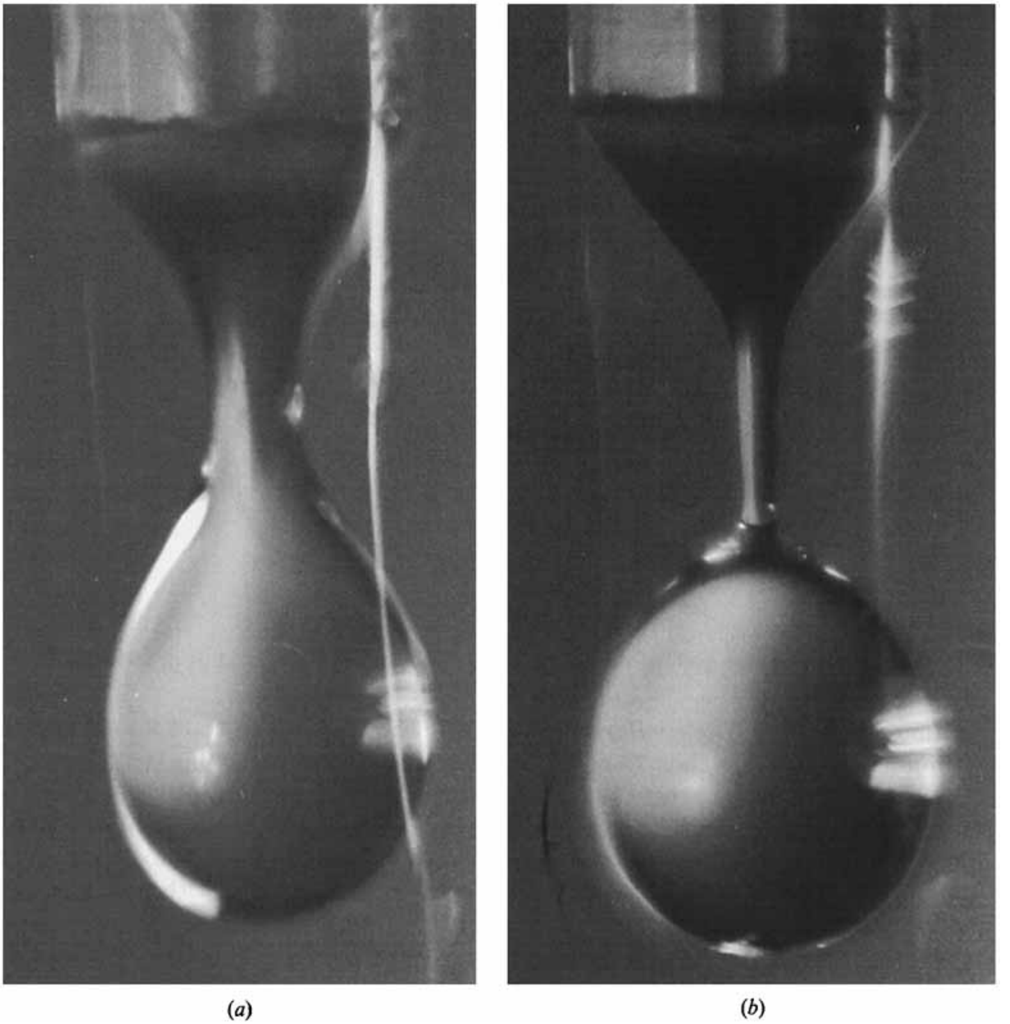

FIGURE 4. (*a*) The initial necking as a drop forms. (*b*) The stage at which necking has formed a columnar liquid bridge.

local configuration also occurs at the moment of bifurcation of the secondary droplet and can be seen in numerous published photographs. Particularly good examples in a liquid–liquid system are shown by Marschall (1985).

2. Experiment

The set of photographs presented here are of water dripping from the end of a glass capillary tube of outer diameter 5.2 mm. The end of the tube provides a scale for the photographs. The water was supplied through a short flexible tube from a burette. The drops were dripping as slowly as possible in order to minimize initial motion in the pendent mass of water.

To obtain clear photographs it was necessary to use a short-duration flash. The flash used had a nomimal duration of 15 μs. It illuminated a white diffusing screen behind the drop. Photographs were taken with a 35 mm camera.

The initial motion of the pendent mass interrupted a light beam. A photo cell then sent a signal to a timing unit which provided a manually variable delay before triggering the flash. Thus all photographs are of different drops: time delays were successively increased. The experiment was in a dark room with the camera shutter open. This has led to a streak of light from the light beam appearing on the photographs. Unfortunately the timing device was insufficiently accurate at the short time intervals required for precise relative times to be assigned to each photograph. The difference in delay time between the closer pairs of photographs is of the order 60 μs. In addition, we assume each drop was identical to its predecessor. It is likely that some of the apparent imprecision of the device may have been due to a scatter of perhaps 5 to 10 μs in the precise moment of bifurcation. A high-speed movie taken at 2000 frames per second, i.e. 500 μs intervals, proved quite inadequate to resolve the motion, but did provide a coarse control on the times quoted above.

3. Description of bifurcation and related events

The sequence of events is illustrated by the photographs in figures 4–9 which are more than eight times life size. This sequence can be divided into the following parts.

3.1. *Necking*

The initial phase of necking, figure 4(*a*), has a smoothly curved surface which gives way to an almost cylindrical columnar bridge between the pendent mass and the nascent drop. This intermediate stage can also be seen in photographs of jets breaking up into drops: the connecting cylinder is described as a 'ligament' by Rayleigh (1891). Progress to this columnar stage is relatively slow with a timescale much greater than a millisecond and the gravity-induced straining is clearly important.

The final necking stage, from figure 4(*b*) to figure 5(*a*), is much shorter with a total time to bifurcation of around 1 ms and with the ultimate contraction where we expect a similarity solution to be relevant taking little more than 100 μs. In this stage we presume surface tension dominates the mechanics.

3.2. *Bifurcation of the main drop*

Figure 5(*b*) shows the instant of bifurcation. The sharp cone on the upper side of the bifurcation point has a half-angle of 9° and blends smoothly with the remaining columnar bridge. On the lower side of the bifurcation point the drop that is formed has a near-spherical shape. Its horizontal diameter is 0.89 of the vertical diameter. Thus we see that close to the bifurcation point there is conical symmetry with a sharp cone touching the smooth surface of the drop which in an appropriately small neighbourhood is equivalent to its tangent plane. In this particular case 0.1 mm is an appropriate lengthscale for this region.

3.3. *Recoil*

Immediately after drop separation the unbalanced surface tension rapidly accelerates liquid in both water bodies. The high initial acceleration, which is singular in the inviscid self-similar model, acts almost like an impact. A round knob forms at the tip of the cone, growing in size without apparent change of shape as might be expected from a similarity solution. Figure 6(*a*) illustrates this stage, but close examination of the negative of figure 5(*b*) reveals, near the limit of resolution, that the tip has a similar shape.

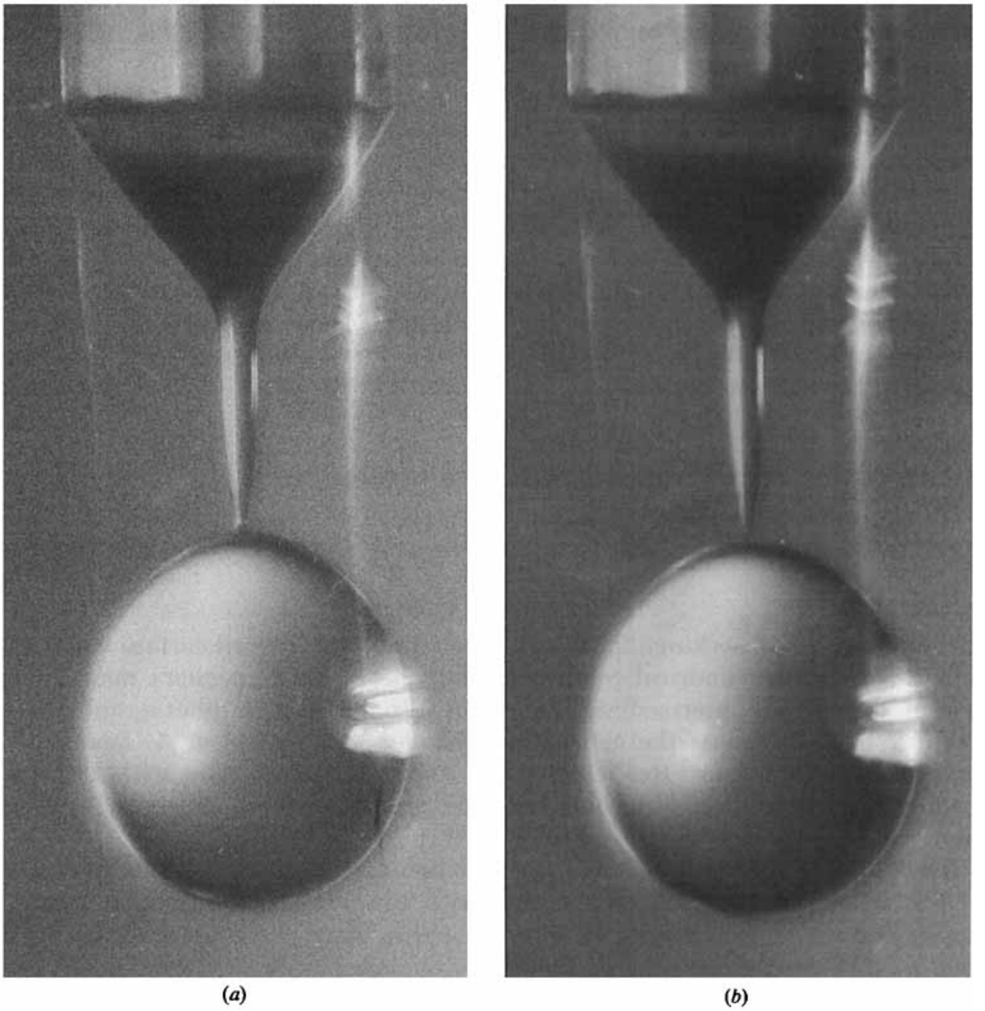

(a) (b)

FIGURE 5. The bifurcation of drop from the columnar liquid bridge: (a) just before, (b) at bifurcation.

The effect on the drop is less clear in these photographs. However, other photographs show recoil occurring with a dimple appearing as the 'release of tension' acts like a point impulse. Later photographs of this series clearly show an apparent flattening of the top of the drop which is in fact the rim of a depression in its surface. The flow visualization experiments of Marschall (1985) show clearly that in his liquid–liquid drop-formation experiment a ring vortex forms within the drop in response to the recoil.

3.4. *Wave generation*

Once the recoil effects propagate up the conical region onto the cylindrical remnant of the liquid bridge much of the original potential energy in the surface of the point cone is converted into wave motion. The illustration in figure 6(*b*) shows small-amplitude waves, which propagate ahead of the disturbance like any other capillary

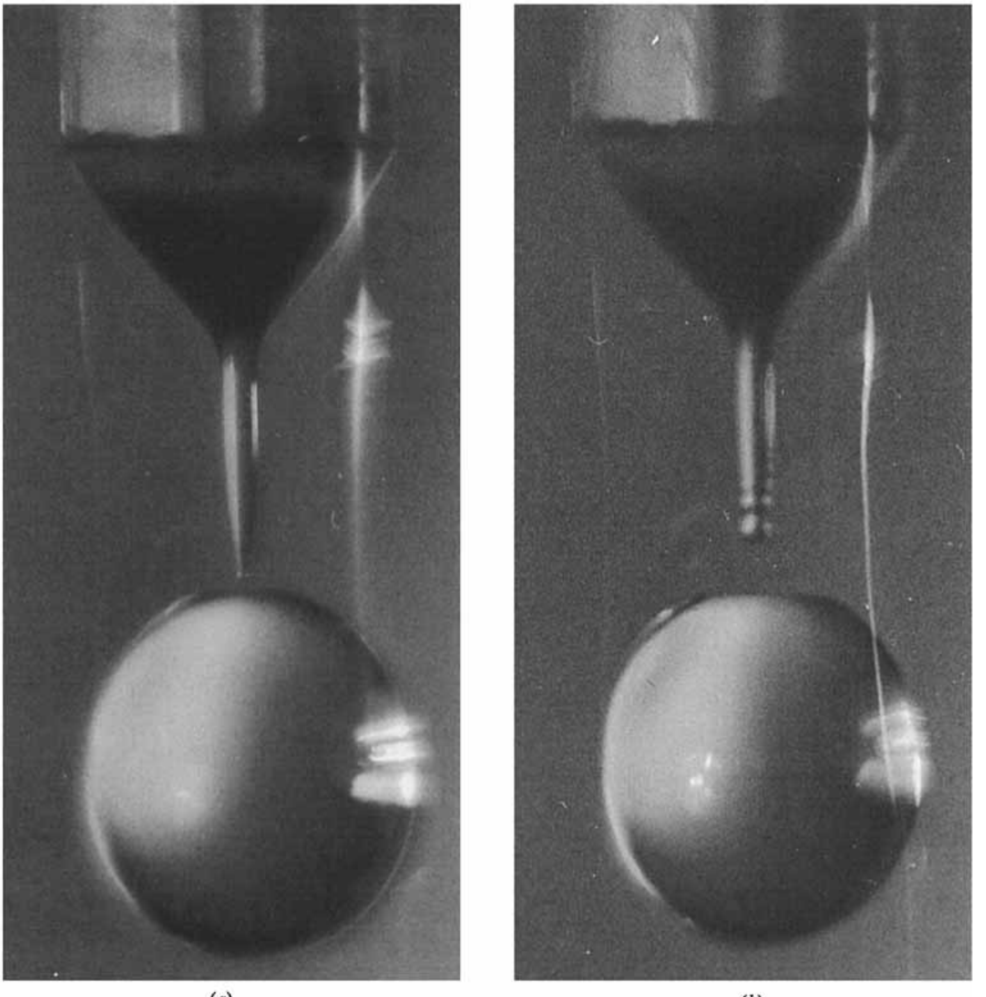

(a) (b)

FIGURE 6. (a) The recoil just after bifurcation. (b) Waves propagating up the column generated by the recoil from bifurcation.

ripples. These are not the growing waves which arise from the instability of a liquid cylinder, but shorter propagating waves.

The cylinder is still shortening so that more energy goes into the wave motion. The knob at the tip grows in size, as may be seen in figure 7(a), and the waves become much steeper. As the figure shows, their troughs become deeper and the crests more rounded, in many ways similar to Crapper's (1957) solution for large-amplitude two-dimensional capillary waves. These waves are better thought of as axisymmetric versions of symmetric waves on thin sheets, for which large-amplitude solutions are given by Kinnersley (1976, see also Hogan 1986). Although such axisymmetric solutions have yet to be analysed it is clear that the steepest waves will have very large curvature in the troughs and are likely to break by touching and trapping a toroidal air bubble. Breaking leads to strong shearing motions which act to dissipate the energy. Our observations made on such waves on fluid jets indicate that they are

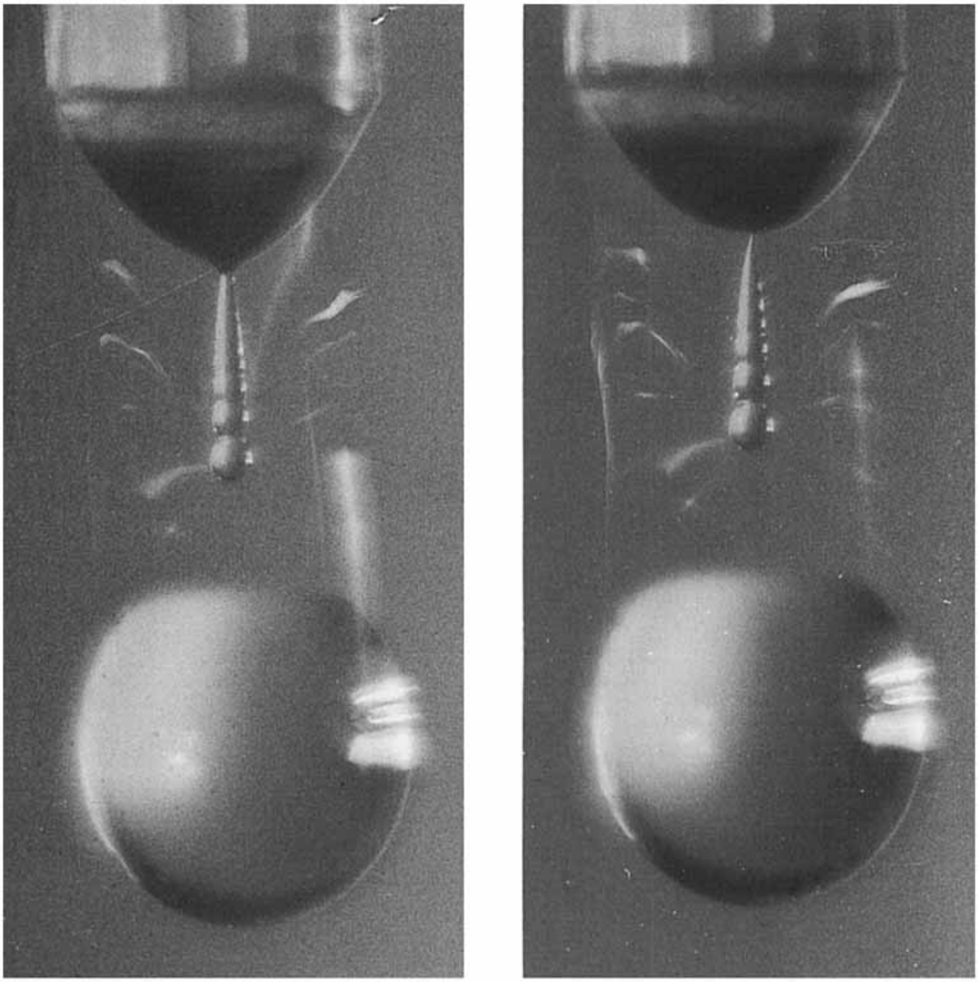

(a) (b)

FIGURE 7. Bifurcation of the secondary droplet from the parent body of water: (a) just before, (b) at bifurcation.

unlikely to cause formation of further drops, except for those extremely small drops that may form from thin liquid films as trapped bubbles burst.

3.5. *Secondary necking and bifurcation*

For this particular experimental configuration a secondary drop forms. The necking and bifurcation can be seen in figure 7 to be almost identical with the initial bifurcation. When large transparent versions of photographs of each bifurcation point are overlaid the overlap of profiles is remarkably close even at a distance from the bifurcation point.

3.6. *Final phase of motion*

Recoil from the secondary bifurcation has a brief self-similar stage which is virtually over in figure 8 (*a*). The brief duration of the self-similar stage is due to waves propagating from the first bifurcation. The waves generated by the secondary recoil mingle with those from the first bifurcation and it is at this stage that the experiment

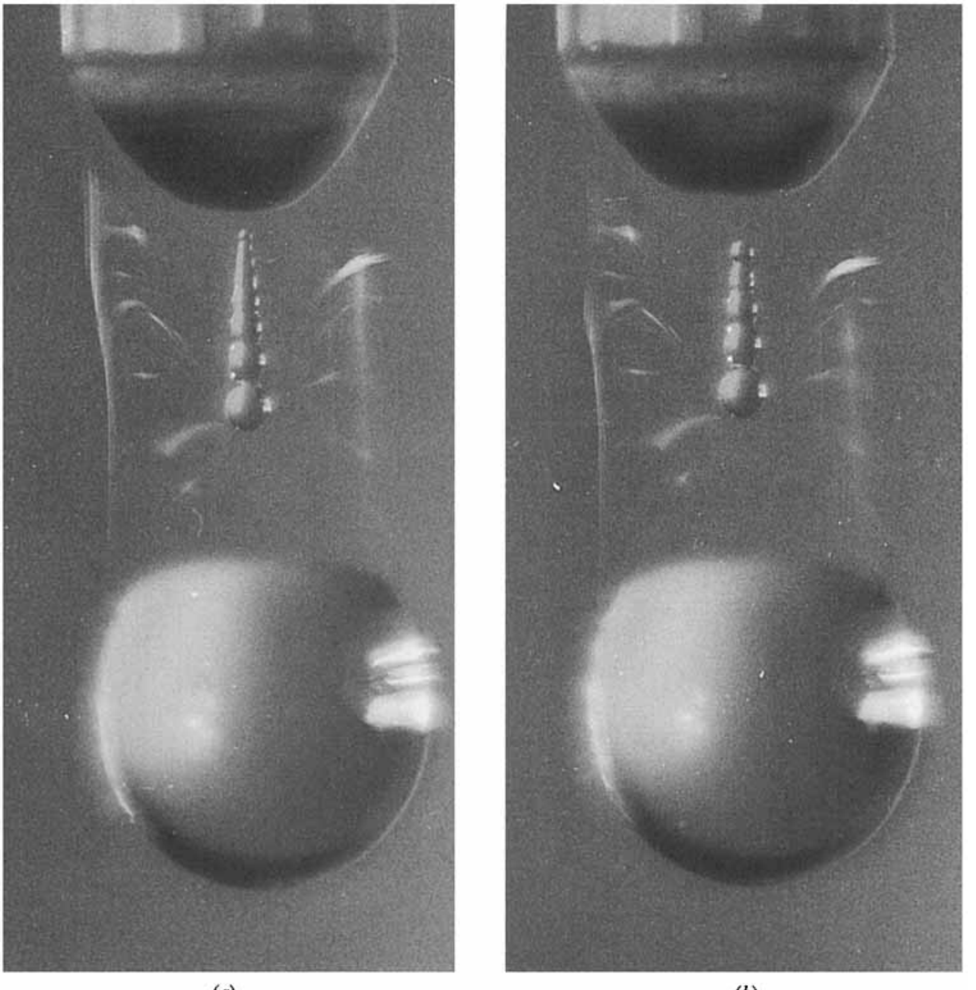

(*a*) (*b*)

FIGURE 8. (*a*) Just after bifurcation of the secondary droplet. (*b*) Large-amplitude waves on secondary droplet.

fails to be entirely repeatable. A range of photographs have been obtained, usually showing three or four major waves on the droplet. Examples are shown in figures 8(*b*), 9(*a*) and 9(*b*). Eventually the droplet contracts towards a spherical shape with wave breaking contributing to dissipation of the excess energy. For example, the line around the lower part of the secondary drop in figure 9(*b*) probably corresponds to a broken wave.

In the photographs of the final stage the strong flattening of the top of the drop and the base of the remaining pendent liquid show continuing effects of recoil. On a longer timescale, these bodies of water oscillate owing to this disturbance.

4. Discussion

One experimental example has been presented here, which immediately raises the question, 'How typical is it?' Other studies of drops, mentioned in the introduction, mostly reproduce photographs at near life size and thus many of the details seen here

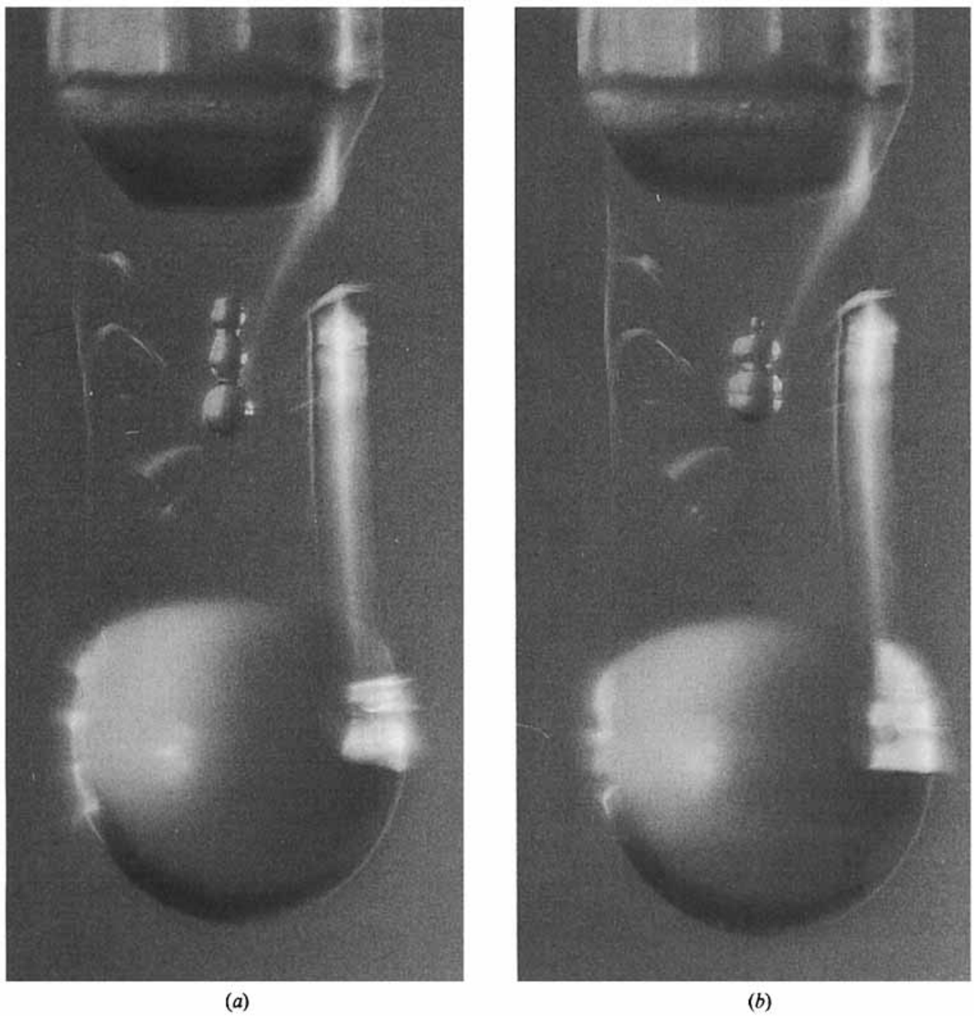

FIGURE 9. Further examples of large-amplitude waves on secondary droplets. Note the line in (b) where a large-amplitude waves may have closed over a toroidal bubble. The flattening of the drop and the remaining pendent mass of liquid is also clear.

are not clear. However, the overall pattern appears to be reproduced. Most studies are for the break-up of a jet. The incipient drops are connected by a thin bridge which is sometimes cylindrical and sometimes bulges when a more substantial secondary drop occurs. Bifurcations occur at the ends of these bridges and show the same strong asymmetry along the axis of rotational symmetry. So far, we have found no photographs of symmetric bifurcation of liquid bridges in air. All these photographs, including a number of liquid–liquid systems, indicate the same strongly asymmetric geometry at bifurcation as is found here. This is despite an initial necking phase, which appears to have appreciable up–down symmetry as seen in figure 4(a).

These experiments suggest that not only is bifurcation described by a similarity solution of the class proposed by Keller & Miksis (1983) but that one particular solution, the one seen at both ends of the columnar bridge in this example, is selected. This solution appears to have a large 'domain of attraction' and this raises the question of how it might be identified mathematically.

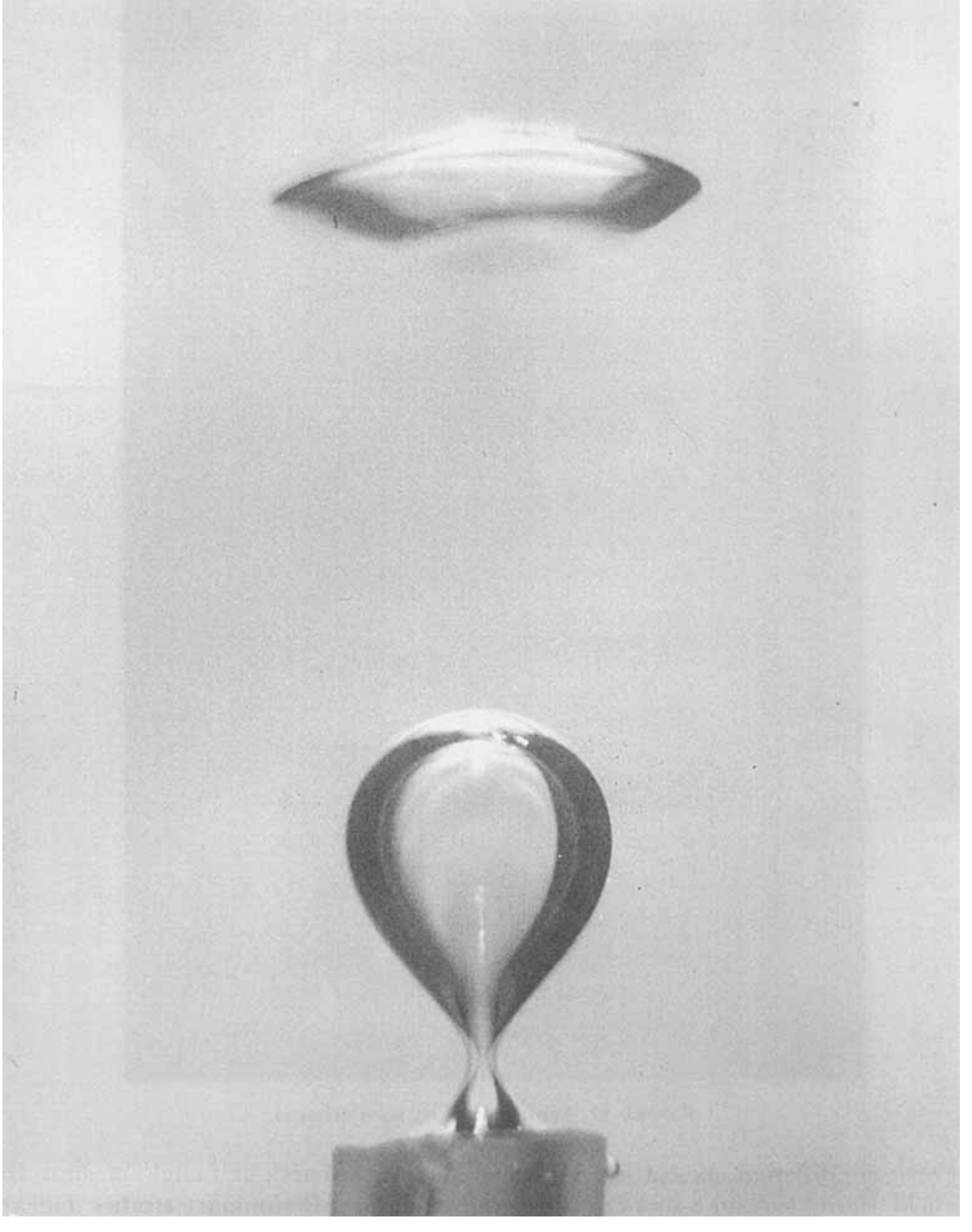

FIGURE 10. Formation of an air bubble in water. Multiple flashes of a stroboscope were used to illuminate this photograph.

The position of bifurcations, at each end of the columnar bridge, hints that a sufficiently strong asymmetry must first be created before bifurcation goes to completion. In addition a mathematical solution must have suitable asymptotic conditions at large distances from the bifurcation point. For an initial wedge these are discussed briefly and incompletely by Keller & Miksis (1983). Further study of this case by Lawrie (1989) shows that the asymptotic form depends strongly on the angle of the wedge, with either wavy or algebraic terms dominating.

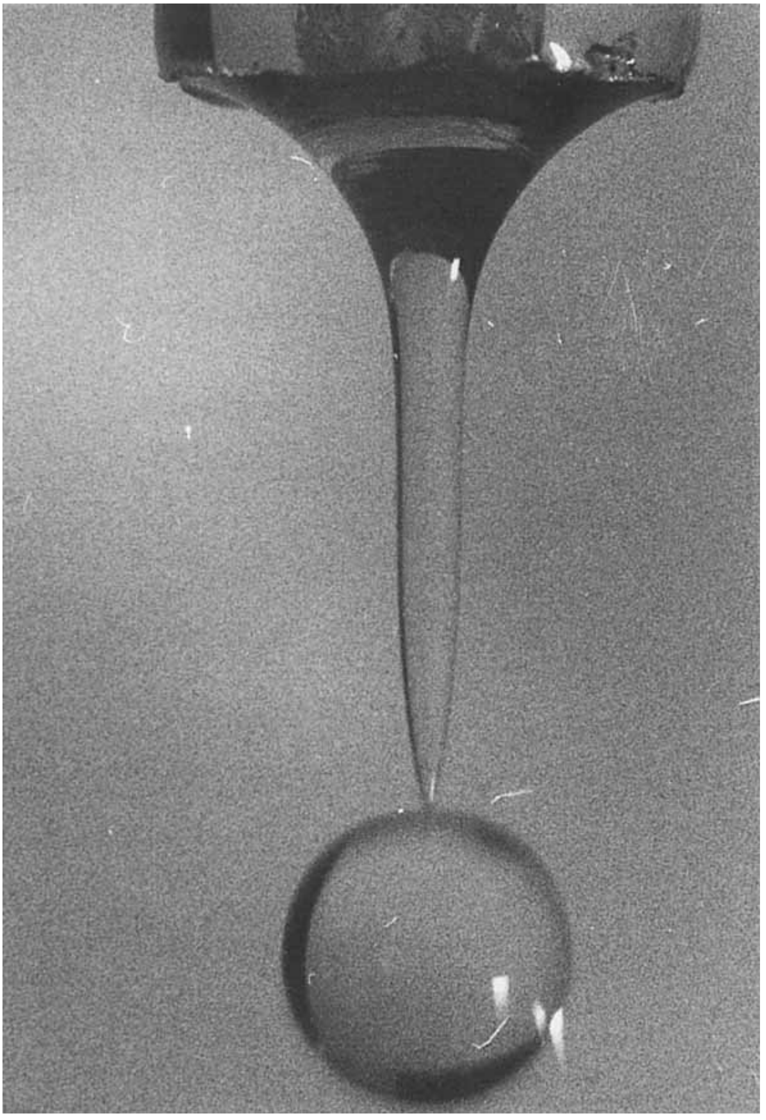

FIGURE 11. Drop formation with ethanol.

Cones are different, except for the planar special case with half angle $\frac{1}{2}\pi$, since the far field cannot sustain a zero-flow first approximation. Preliminary studies indicate that source-like flows, i.e. velocity potential inversely proportional to distance, provide a suitable and easily understood far field. In addition wave terms must be expected. For times, $t < 0$, the waves are converging on the bifurcation point. This property of a 'wavy' similarity solution appears to contradict causality. How can waves be generated with precisely the correct behaviour to converge on a future point in space–time? The natural corollary of this observation is that any solution describing the approach to bifurcation must be 'non-wavy'. This has the implication that there may only be a small number of possible non-wavy similarity solutions. They may be thought of as eigenfunctions with the cone angles on each side of the bifurcation point taking the place of the eigenvalue. That is if (α, β) are the two cone

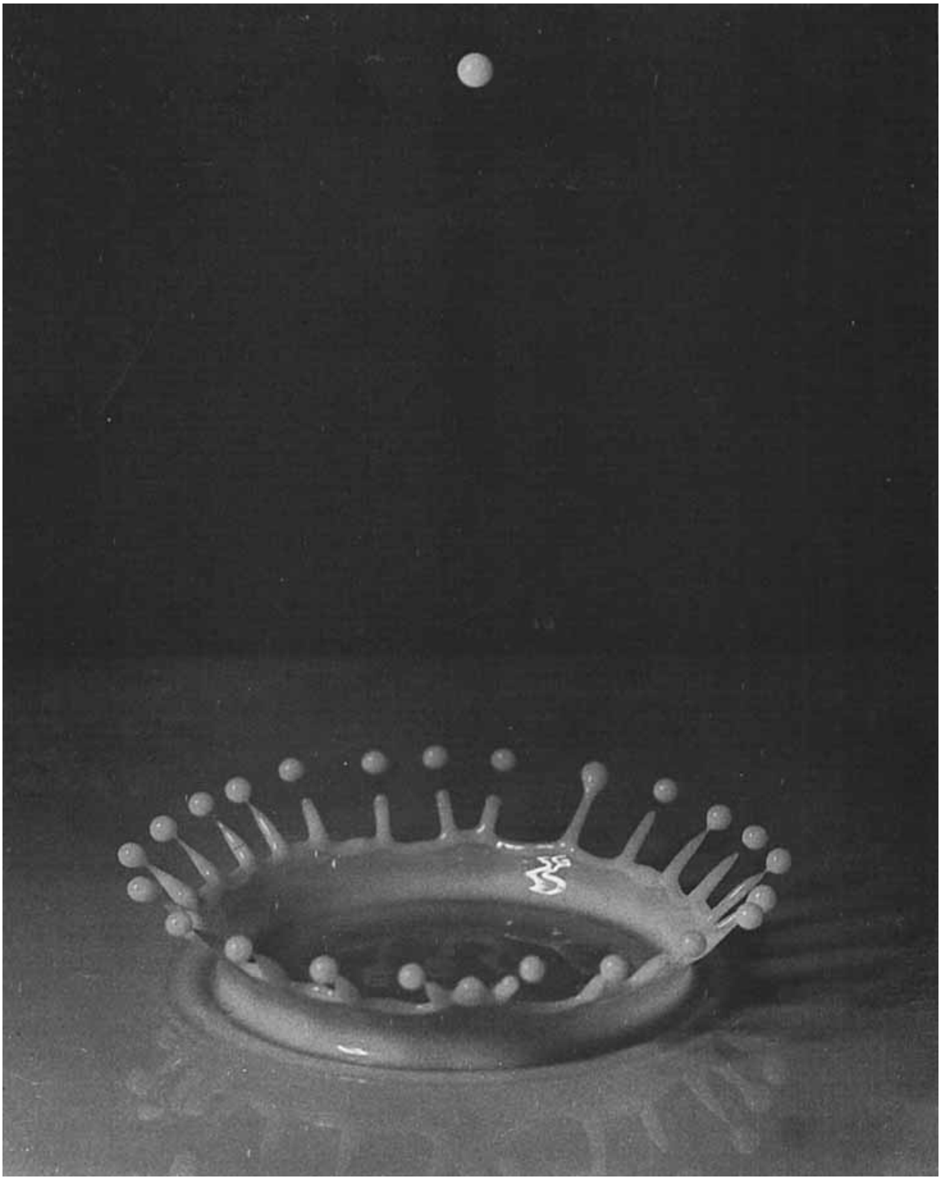

FIGURE 12. Drop formation in the splash arising from a drop of milk falling into a thin layer of milk (courtesy of Harold Edgerton).

angles then only certain 2 vectors, (α_i, β_i) give 'non-wavy' solutions, e.g. figures 5(*b*) and 7(*b*) correspond to values of approximately (90°, 9°) and (9°, 90°).

The above discussion has assumed the dominance of surface tension, but other factors which can influence bifurcation should be considered. One dominant factor which appears in a self-similarity formulation of the problem is the density ratio. To shed a little light on this parameter a brief experiment was made with air bubbles. A stream of bubbles forming at the mouth of a tube were photographed with stroboscopic illumination. The moment of bifurcation proved very hard to catch, but the photograph in figure 10 taken with four successive flashes shows that bifurcation in this case is more nearly symmetrical. However, measurement of an enlargement gives a pair of cone angles (34°, 42°) which are not equal. A large field of view is shown in figure 10 to include the previous bubble which shows the strong deformation which arises from the recoil at bifurcation. Experiments with different liquids showed very similar behaviour. For example, ethanol has a surface tension 30% that of water, yet the only significant differences are a longer column and a drop of about half the diameter of a water drop, see figure 11. Edgerton's photographs of milk drops in McDonald (1954) also indicate very similar behaviour.

Gravity initiates drop formation in this case. It could continue to influence the flow either directly or through the overall rate of strain of the drop motion. The timescale of bifurcation, τ, is $O(100\ \mu s)$. The corresponding dimensionless ratio giving the importance of gravity relative to surface tension is $g(\tau^4\rho/T)^{\frac{1}{3}} \approx 10^{-3}$. The overall rate of strain, A, due to the motion of the drop is about 20 s^{-1} giving $A\tau \approx 2\times 10^{-3}$. Both of these dimensionless numbers are sufficiently small that we do not expect gravity or the rate of strain to affect flow close to bifurcation. Both viscosity and compressibility are discussed in the introduction.

5. Conclusion

The photographs of drops as they drip presented here were taken in response to Keller & Miksis (1983) suggestion that flow near bifurcation may be described by self-similar solutions. The photographs give some support to that view, but in addition lead to the hypothesis that only particular self-similar solutions are selected by the dynamical evolution. It is suggested that this is because the approach to bifurcation cannot support waves which are approaching the bifurcation point in a self-similar manner. Since the self-similar flows have singular velocities, etc. at the instant of bifurcation, there may be some interest in studying the effect of such extreme conditions on fluid properties, on material dissolved or suspended in the liquid and on electrical properties such as charge separation. Another notable feature, which appears to be common to other examples of drop creation is the development of a thin bridge, columnar in this case. This appears to govern the location of bifurcations at the junctions of the bridge with the larger liquid masses.

Large-amplitude surface waves are seen on the secondary droplet and its precursor. These appear to be consistent with the properties to be expected by analogy with two-dimensional solutions.

Finally, in figure 12 another example is presented where drop formation comes after narrow liquid bridges break at their ends with sharp points: the 'coronet' of splash plus drops that occurs after a drop falls onto a thin layer of liquid.

The assistance of Dr M. E. R. Walford in supervising the experiments, and of the United Kingdom Science and Engineering Research Council in providing support to initiate theoretical study of these experiments are acknowledged.

REFERENCES

Chaudhary, K. C. & Maxworthy, T. 1980*a* The nonlinear capillary instability of a liquid jet. Part 2. Experiments on jet behaviour before droplet formation. *J. Fluid Mech.* **96**, 275–286 + 2 plates.

Chaudhary, K. C. & Maxworthy, T. 1980*b* The nonlinear capillary instability of a liquid jet. Part 3. Experiments on satellite drop formation and control. *J. Fluid Mech.* **96**, 287–297 + 10 plates.

CHAUDHARY, K. C. & REDEKOPP, L. G. 1980 The nonlinear instability of a liquid jet. Part 1. Theory. *J. Fluid Mech.* **96**, 257–274.

CRAPPER, G. D. 1957 An exact solution for progressive capillary waves of arbitrary amplitude. *J. Fluid Mech.* **2**, 532–540.

EDGERTON, H. E., HAUSER, E. A. & TUCKER, W. B. 1937 Studies in drop formation as revealed by the high-speed motion camera. *J. Phys. Chem.* **41**, 1017–1028.

GOEDDE, E. F. & YUEN, M. C. 1970 Experiments on liquid jet instability. *J. Fluid Mech.* **40**, 495–511.

HOGAN, S. J. 1986 Highest waves, phase speeds and particle trajectories of nonlinear capillary waves on sheets of fluid. *J. Fluid Mech.* **172**, 547–563.

KELLER, J. B. & MIKSIS, M. J. 1983 Surface tension driven flows. SIAM *J. Appl. Maths* **43**, 268–277.

KINNERSLEY, W. 1976 Exact large amplitude capillary waves on sheets of fluid. *J. Fluid Mech.* **77**, 229–241.

LAWRIE, J. B. 1989 Surface tension driven flow in a wedge. *Q. J. Mech. Appl. Maths* (to appear).

MCDONALD, J. E. 1954 The shape of raindrops. *Sci. Am.* **190**, Feb., 64–68.

MARSCHALL, E. 1985 Zur Strömungsmechanik während der Tropfenbildung in flüssigen Zweiphasen. *Ver. Deutscher Ingen. Forschungscheft* **632**, 13–17.

MESEGUER, J. & SANZ, A. 1985 Numerical and experimental study of the dynamics of axisymmetric slender liquid bridges. *J. Fluid Mech.* **153**, 83–101.

PITTS, E. 1974 The stability of pendent liquid drops. Part 2. Axial symmetry. *J. Fluid Mech.* **63**, 487–508.

RAYLEIGH, LORD 1891 Some applications of photography. *Nature* **44**, 249–254 (in *Scientific Papers* (1902) vol. 3, pp. 441–451, with better reproduction of photographs).

STONE, H. A., BENTLEY, B. J. & LEAL, L. G. 1986 An experimental study of transient effects in the break-up of viscous drops. *J. Fluid Mech.* **173**, 131–158.

STONE, H. A. & LEAL, L. G. 1989 Relaxation and break-up of an initially extended drop in an otherwise quiescent fluid. *J. Fluid Mech.* **198**, 399–427.

TAYLOR, G. I. 1932 The viscosity of a fluid containing small drops of another fluid. *Proc. R. Soc. Lond.* A **138**, 41–48 (*Scientific Papers* vol. 4, pp. 101–106).

WILSON, S. D. R. 1988 The slow dripping of a viscous fluid. *J. Fluid Mech.* **190**, 561–570.

WORTHINGTON, A. M. 1897 Impact with a liquid surface, studied by the aid of instantaneous photography. *Phil. Trans. R. Soc. Lond.* A **189**, 137–148 + 8 plates.

WORTHINGTON, A. M. 1908 *A Study of Splashes.* Longmans. xii + 129 pp.